Journal of Computer and Communications, 2016, 4, 28-34
Published Online March 2016 in SciRes. http://www.scirp.org/journal/jcc
http://dx.doi.org/10.4236/jcc.2016.43005

Scientific Research Publishing

A Study on the Influence of Luminance L* in the L*a*b* Color Space during Color Segmentation

Rodolfo Alvarado-Cervantes[1], Edgardo M. Felipe-Riveron[2*], Vladislav Khartchenko[1], Oleksiy Pogrebnyak[2]

[1]Centro de Investigaciones Teóricas, Facultad de Estudios Superiores Cuautitlán, Universidad Nacional Autónoma de México, Primero de Mayo S/N Campo 1 Cuautitlán Izcalli, México
[2]Centro de Investigación en Computación, Instituto Politécnico Nacional, Juan de Dios Batiz w/n, Col. Nueva Industrial Vallejo, P.O. 07738, México
Email: *edgardo@cic.ipn.mx, vlad@unam.mx

Received 15 January 2016; accepted 26 February 2016; published 2 March 2016

Abstract

In this paper an evaluation of the influence of luminance L* at the L*a*b* color space during color segmentation is presented. A comparative study is made between the behavior of segmentation in color images using only the Euclidean metric of a* and b* and an adaptive color similarity function defined as a product of Gaussian functions in a modified HSI color space. For the evaluation synthetic images were particularly designed to accurately assess the performance of the color segmentation. The testing system can be used either to explore the behavior of a similarity function (or metric) in different color spaces or to explore different metrics (or similarity functions) in the same color space. From the results is obtained that the color parameters a* and b* are not independent of the luminance parameter L* as one might initially assume.

Keywords

Color Image Segmentation, CIELAB Color Space, L*a*b* Color Space, Color Metrics, Color Segmentation Evaluation, Synthetic Color Image Generation

1. Introduction

Image segmentation consists of partitioning an entire image into different regions, which are similar in some predefined manner. It is an important and difficult task in image analysis and processing. All subsequent steps, such as object recognition depend on the quality of segmentation [1].

For some time the development of segmentation algorithms attracted remarkable consideration compared with the relatively fewer efforts on their evaluation and characterization [2]-[5]. Since none of the proposed automatic segmentation algorithms published is generally applicable to all types of images and different algorithms are not equally suitable for particular applications, the performance evaluation of segmentation algorithms and its

*Corresponding author.

How to cite this paper: Alvarado-Cervantes, R., Felipe-Riveron, E.M., Khartchenko, V. and Pogrebnyak, O. (2016) A Study on the Influence of Luminance L* in the L*a*b* Color Space during Color Segmentation. *Journal of Computer and Communications*, **4**, 28-34. http://dx.doi.org/10.4236/jcc.2016.43005

characterization are very important subjects in the study of segmentation [3] [5].

Perceptual uniform color spaces such as L*a*b*, with the Euclidean metric to quantify color distances are commonly used in color image segmentation of natural scenes using histogram based or clustering techniques among others [1].

To evaluate the segmentation performance of the Euclidian metric in the L*a*b color space we designed a system that generated synthetic color images, with its associated ground truth (GT), and evaluated the results with Receiver operating characteristics (ROC) curves [7]. The synthetic images where designed to evaluate the efficiency of achieved color information from given segmentation algorithms and are explained in detail in Section 3. A comparative study with an adaptive color similarity function defined as a product of Gaussian functions in a modified HSI color space [6] is presented in Section 4. Conclusions are presented in Section 5.

2. Previous Works

The first comprehensive survey on evaluation methods of image segmentation is presented in [2]. It brings a coherent classification of existing methods at the time. An up to date of 5 years of progresses in the subject is presented in [3] after the first survey. Another actualization is presented 5 years later [5], embracing together the principal methods of segmentation evaluation available until 2007.

In [4] a way to design synthetic images and a corresponding GT for evaluating segmentations algorithms is presented. They introduce a general framework and general design considerations. They also present an evaluation system for generating synthetic gray level images taking into account their design considerations.

3. Design of Synthetic Images for Benchmark Testing

In [4] the authors present three important design considerations for creating synthetic images: 1) Synthetic images should be appropriate for a quantitative study and should allow objective evaluations of their properties; 2) The synthetic images should reflect the main features of real images, *i.e*. corruption factors, such as noise and blurring, variation of parameters such as size, shape, etc.; 3) The system should allow the generation of images with progressive variations of each parameter. In this way the study of the influence of each individual parameter is possible.

Comparative tests between an adaptive color similarity function [6] and the Euclidean metric in the L*a*b* color space [8] were performed. The manner in which the tests were implemented is as follows:

In the case of the L*a*b* color space, the RGB image was previously transformed to L*a*b* color space discarding in all cases the luminance L* in order to calculate the Euclidean distance on the planes a*b* (color information) independently of the illumination.

Then the centroid (average of the values a* and b*) representing the colors of the figure and the background in the color space L*a*b* was calculated. Details are shown in [8]. For the adaptive similarity function [6] the following steps were performed:

1) Samples of both background and figure were taken, from which centroid and standard color dispersion were calculated. Details can be consulted in [6]
2) The 24-bit RGB image (true color) was transformed to a modified HSI color space.
3) For each pixel, the similarity function to the centroids of figure and background was calculated creating two color similarity images (CSI) [6].
4) Each pixel of the RGB image was classified by calculating the maximum value for each pixel position between the CSI images of the figure and that of the background.

The base shape of the synthetic test image was created with the following features:

1) Concave and convex sections in order to make it more representative of real images, such as natural flowers. 2) Extreme omnidirectional curvature in the entire image to hinder obtaining the edges applying mask edge detectors. 3) The object was centered in the image.

The resulting flower-shaped object in the image is considered as the object of interest and as the ground truth GT in all subsequent tests (**Figure 1** left).

In addition to this object of interest, several features were imposed in order to hinder its color-based segmentation:

1) Low contrast. The contrast between the object and the background in all images was very low for an observer, including some in which at a first glance the user cannot see the difference (e.g. Flower 5 in **Figure 2**).

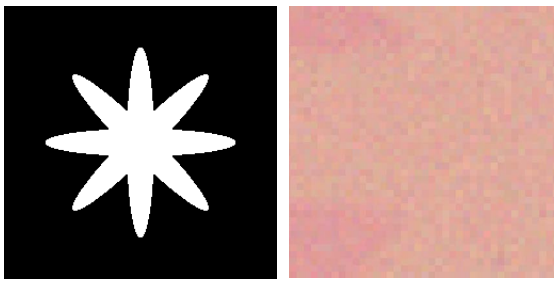

Figure 1. Flower-shaped ground truth (left) and an image zoomed showing the Gaussian noise introduced (right).

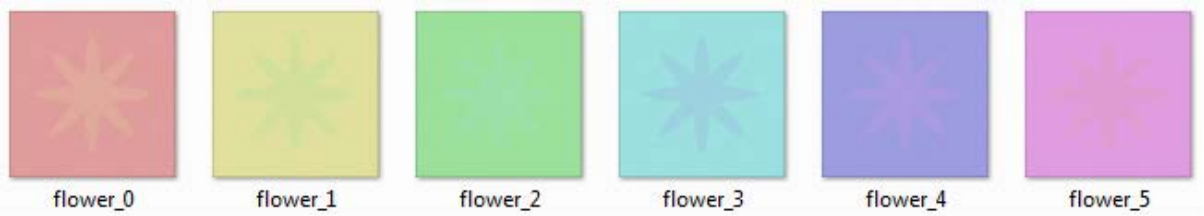

Figure 2. Testing with low saturation with delta in HUE.

The difference between the color characteristics of the object of interest and the background is called Delta by us and occurs at different directions of the HSI space. The tests were performed in color quadrants 0, 60, 120, 180, 240 and 300 degrees.

2) Blurred edges with an average filter. A mean filter of size 3 × 3 pixels was applied to the whole image in order to blur the corners and to make detection of the object more difficult; this was done before the introduction of Gaussian noise.

3) Introduction of Gaussian noise with SNR value = 1 (**Figure 1** right). The noise was applied to each of the RGB channels individually, and later we assembled the channels to create the RGB color image with noise. **Figure 1** right shows an example.

The basic colors selected for both figure and background were based on maintaining constant intensity to 0.5 and saturation to 0.3 and only varying the hue. Hue was selected as the parameter because its change integrates the three RGB color channels together, making it more difficult to be processed by extending grayscale techniques to each color channel, thus forcing the segmentation algorithms in evaluation to use the color information holistically.

Samples of pixels corresponding to the figure were obtained by two squares of 2 × 2 pixels starting at the pixel (84, 84) and (150, 150). Samples for background pixels were obtained by two squares of 2 × 2 pixels starting at pixel (15, 15) and (150, 180).

The images were generated in the sectors 0, 60, 120, 180, 240 and 300 degrees corresponding to the images flower_0, flower_1 … flower_5 (**Figure 2**). To these test images we later applied to each one a faded shadow in increments of 10% in each step.

A shadow fading was applied to all noisy blurred images with the light center in the fixed coordinates (150, 150) in images of 256 × 256 pixels. It was applied gradually with 10% increments in each step. **Figure 3** shows this for Flower 0.

4. Results and Discussion

In this section we show the results of TP (true positives) and FP (false positives) plotted against the level of shadow fading, representing each 10% step of increment. The first position means no shadow and position 11 means 100% shadow fading. All the images had the same post-processing: elimination of areas smaller than 30 pixels and a morphological closing with a circular structuring element of radius equal to two pixels.

The results of the application with the solution given by [6] of the color image segmentation with a different level of shadow fading (shown in every even row) compared with those obtained with the Euclidean metric in the L*a*b* rejecting L* (shown in every odd row) are included in **Figure 4** for each color quadrant (0˚, 60˚,

Figure 3. Example in color quadrants with a faded shadow applied at 0 degrees.

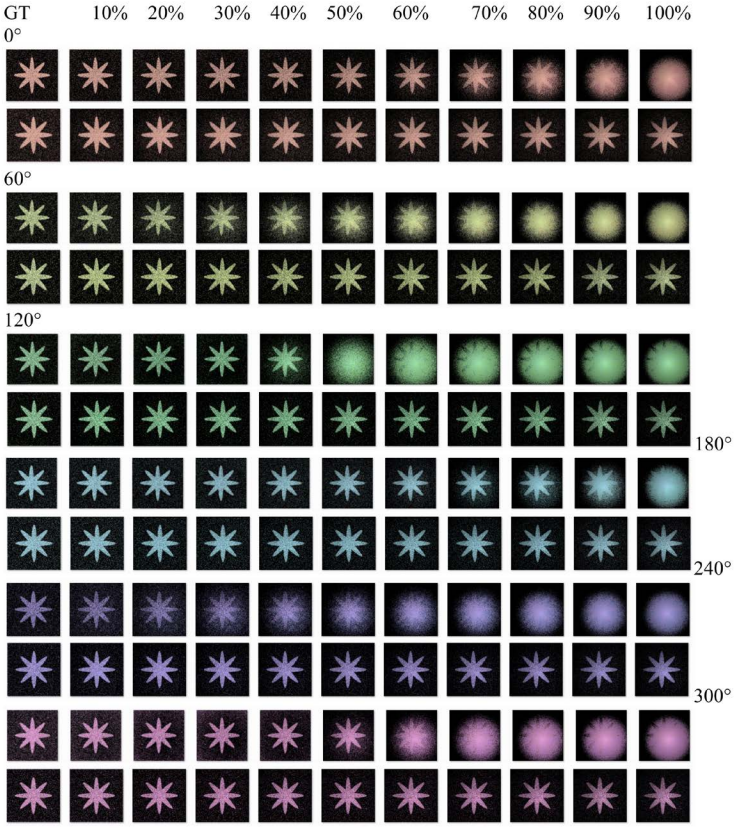

Figure 4. Results of the color segmentation achieved between the Euclidean metric of a* and b* (top rows of each color) and the adaptive color similarity function (bottom rows of each color), for each color quadrant (0˚, 60˚, 120˚, 180˚, 240˚ and 300˚) and at 10% increments of shadow fading in each step.

120˚, 180˚, 240˚ and 300˚) and at 10% increments of the shadow fading.

As it is shown in the graphs of **Figure 5** and in coincidence with the visual analysis of the corresponding flower (**Figure 4**), segmentation failures in the L*a*b* space (right) start at different levels of faded shadow, whereas the adaptive color similarity function [6] is practically immune to the faded shadow (left).

We can see three general trends in the FP behavior in **Figure 5** right (See **Table 1**): 1) Increase in an angle of approximately 45˚ in cases of Flower 0 and Flower 3 (with diamond marker); 2) Slowly and progressively increases in cases of Flower 1 and Flower 4 (with square marker) and 3) Sharply increases in cases of Flower 2 and Flower 5 (with circular marker). The behavior is repeated every 180 degrees and coincides with the opponent color positions (yellow-blue for example).

Figure 6 shows details of the curves related to TP and FP of the color similarity function [6], with the following color code: Flower 0 (blue), Flower 1 (green), Flower 2 (red), Flower 3 (cyan), Flower 4 (purple) and Flower 5 (yellow). Variations in curves are lower than 1%.

To obtain a representative ROC curve illustrating behavior of the Euclidean metric in the L*a*b* space (rejecting L*) compared to the color similarity function [6] in all color sectors under study, we calculated the average TP and FP for all color flowers, obtaining the results shown in **Figure 7**.

In the ROC curve corresponding to the average of TP and FP of all flowers, it can be seen that the results of the adaptive similarity function are maintained in the high efficiency area (coordinate 0, 1) while the color

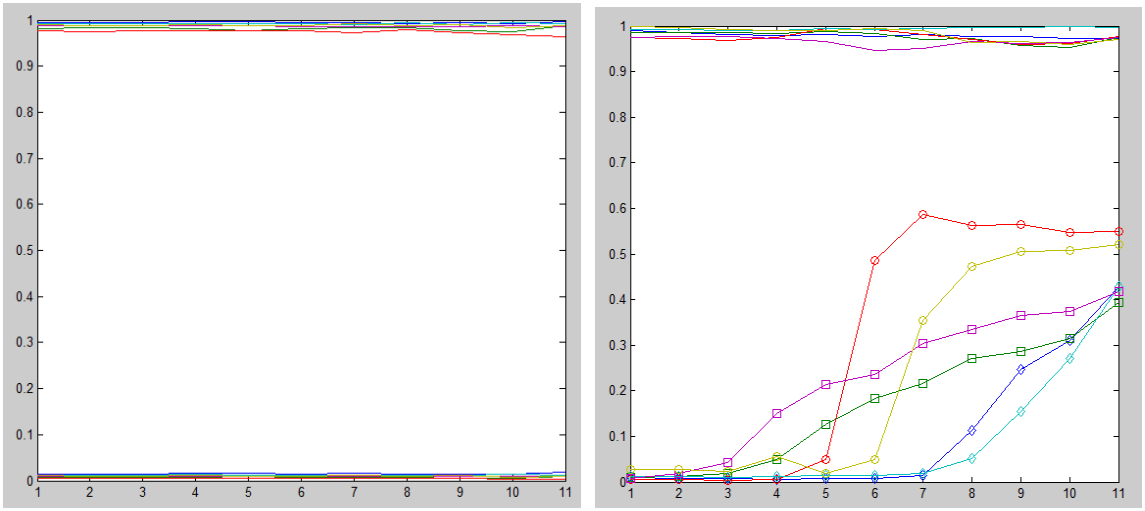

Figure 5. Plots of the color similarity function [6] (left) and the Euclidean metric in L*a*b* rejecting L* (right).

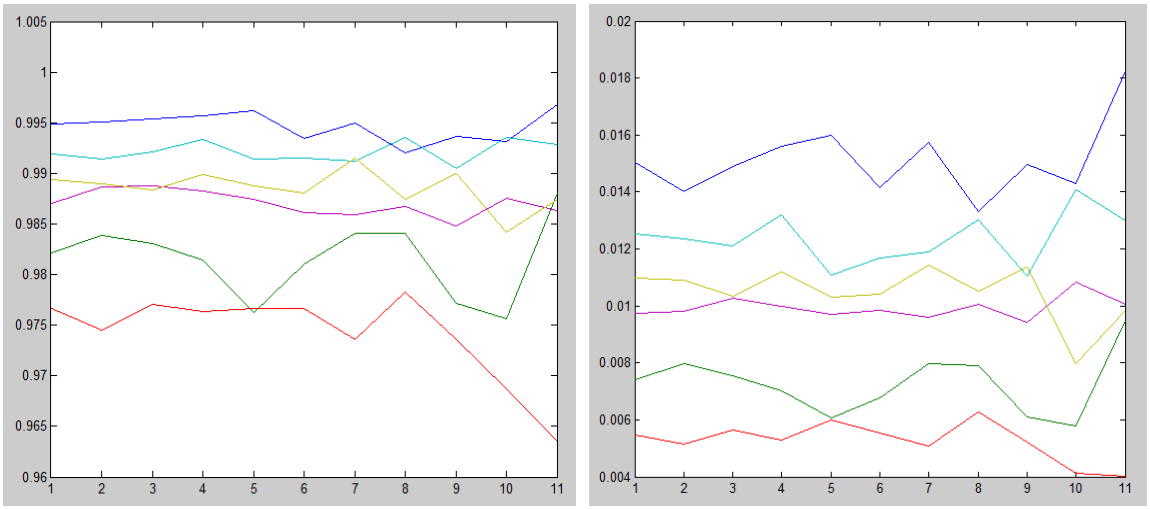

Figure 6. Details of TP (left) and FP (right) of the color similarity function [6].

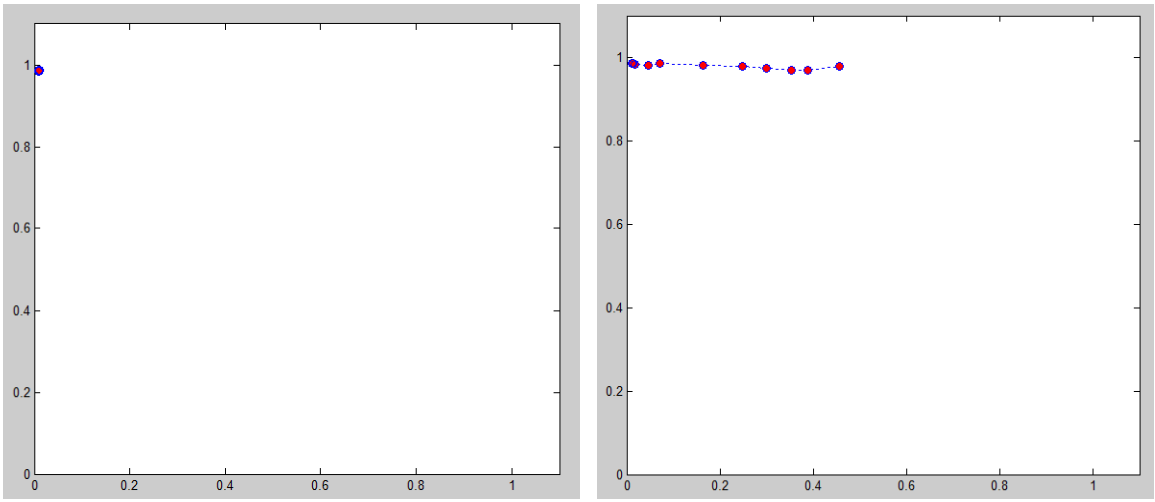

Figure 7. ROC curve of the color similarity function [6] (left) and the Euclidean metric in the L*a*b* rejecting L*.

Table 1. Observations concerning the behavior of the plot curves of the two color metrics.

Flower	Line Color	Euclidean metric in L*a*b* rejecting L*	Color similarity function [6]
0	Blue	60% (position 7) Increases at 45˚	Immune
1	Green	30% (position 4) Increases slowly and progressively	Immune
2	Red	40% (position 5) Sharply increases	Immune
3	Cyan	70% (position 8) Increases at 45˚	Immune
4	Purple	20% (position 3) Increases slowly and progressively	Immune
5	Yellow	50% (position 6) Sharply increases	Immune

segmentation in L*a*b* space progressively moves away from the high efficiency area.

The L*a*b* results keep stable initially and later slowly and progressively moves to the upper right area of the ROC curve that can be thought of as the "liberal" side (coordinate 1, 1) as they make positive classifications, and, although there is weak evidence that almost all positives were classified properly, they have a high rate of false positives.

5. Conclusions

Regarding the evaluation of the color segmentation method with really difficult conditions, we can notice that the adaptive color similarity function performed well in all tests and remained close to the high efficiency zone of the ROC curves (coordinates 0, 1) without noticeable changes when the level of faded shadow increases as shown in the corresponding PLOT curves.

The segmentation algorithm using the L*a*b* color space and discarding L* in calculating the Euclidean distance, suffered errors in all cases. It manifested in different degrees and at different levels of faded shadow (20% to 80%). Three types of trends or recurring symmetries can be noticed in sectors with 180 degrees of difference: 1) Rise of the curve gradually (Flowers 1 and 4); 2) Rise abruptly (Flowers 2 and 5), and 3) Increase near at 45˚ angle (Flowers 0 and 3).

As it can be seen from the results of both direct segmentation, and from PLOT & ROC curves, that the adaptive color similarity function in all cases exceeded the Euclidean distance in color space L*a*b* and discarding L*. The similarity function segmentation method performed well in all cases with rates higher than 95% of true positives (TP) and false positive (FP) rate less than 3% on average.

According to the experiment results we believe that keeping high values of TP (true positive) increased only from the FP (false positive) is due to the position of the center of the shadow fading in (150, 150). If this position is moved away from the object of interest, we can reduce the quantity of TP.

For future work we wish to evaluate different color zones like with different saturations, gray images, and with delta saturation among others. Our testing system can be used either to explore the behavior of a similarity function (or metric) in different color spaces or to explore different metrics (or similarity functions) in the same color space. Instead of exchanging color spaces in the experiments, it would only be necessary to exchange the metric or the similarity function.

It can be noticed that the non-consideration of the luminance parameter L* in calculating Euclidean distance (in each pixel of the object or of the background) did not made it immune to changes in lighting; so simple shadow can alter the quality of the results, concluding from them that the parameters a*b* from the color space L*a*b* are not independent of the L* parameter as one might suppose.

Acknowledgements

The authors of this paper wish to thank the Centro de Investigaciones Teóricas, Facultad de Estudios Superiores Cuautitlan (FES-C); Universidad Nacional Autónoma de México (UNAM), México; PAPIIT IN112913 and PIAPIVC06, UNAM; Centro de Investigación en Computación (CIC); Secretaría de Investigación y Posgrado (SIP); Instituto Politécnico Nacional (IPN), México, and CONACyT, México, for their economic support to this work.

References

[1] Plataniotis, K.N. and Venetsanopoulos, A.N. (2000) Color Image Processing and Applications. Springer, Berlin Heidelberg Germany, 354 p. http://dx.doi.org/10.1007/978-3-662-04186-4

[2] Zhang, Y.J. (1996) A Survey on Evaluation Methods for Image Segmentation. *Pattern Recognition*, **29**, 1335-1346. http://dx.doi.org/10.1016/0031-3203(95)00169-7

[3] Zhang, Y.J. (2001) A Review of Recent Evaluation Methods for Image Segmentation. *Proceedings of the* 6*th International Symposium on Signal Processing and Its Applications*, 148-151.

[4] Zhang, Y.J. and Gerbrands, J.J. (1992) On the Design of Test Images for Segmentation Evaluation. *Proceedings EUSIPCO*, **1**, 551-554.

[5] Zhang, Y.J. (2006) A Summary of Recent Progresses for Segmentation Evaluation. In: Zhang Y.J. Advances in Image and Video Segmentation. IGI Global Research Collection, Idea Group Inc (IGI), 423-439.

[6] Alvarado-Cervantes, R., Felipe-Riveron, E.M. and Sanchez-Fernandez, L.P. (2010) Color Image Segmentation by Means of a Similarity Function. In: Alvarado-Cervantes, R., Felipe-Riveron, E.M., Sánchez-Fernandez, L.P., Bloch, I. and Cesar Jr., R.M., Eds., 15*th Iberoamerican Conference on Pattern Recognition*, *CIARP*, Sao Paulo, Brazil, 8-11 November 2010, 319-328. Springer, Heidelberg.

[7] Fawcett, T. (2006) An Introduction to ROC Analysis. *Pattern Recognition Letters*, **27**, 861-874. http://dx.doi.org/10.1016/j.patrec.2005.10.010

[8] http://www.mathworks.com/help/images/examples/color-based-segmentation-using-the-l-a-b-color-space.html (Revised on April 27, 2015)